

## CFD MODELING OF GAS-LIQUID FLOW AND HEAT TRANSFER IN A HIGH PRESSURE WATER ELECTROLYSIS SYSTEM

V. Agranat<sup>1</sup>, S. Zhubrin<sup>2</sup>, A. Maria<sup>3</sup>, J. Hinatsu<sup>1</sup>, M. Stemp<sup>1</sup> and M. Kawaji<sup>3</sup>

<sup>1</sup>Hydrogenics Corporation, 5985 McLaughlin Road, Mississauga, ON L5R 1B8, Canada

<sup>2</sup>Flowsolve Limited, 40 High Street, Wimbledon Village, London, SW19 5AU, UK

<sup>3</sup>University of Toronto, Department of Chemical Engineering and Applied Chemistry, 200 College Street, Toronto, ON M5S 3E5, Canada

E-mail: [vagranat@hydrogenics.com](mailto:vagranat@hydrogenics.com)

### ABSTRACT

A high-pressure water electrolysis system has been investigated numerically and experimentally. The advanced CFD model of two-phase flow, which calculated the 3D distributions of pressure, gas and liquid velocities and gas and liquid volume fractions, has been developed to account for all the major components in the system, and appropriate constitutive equations for two-phase flow parameters were selected for various parts of the system, such as the cell stack, riser, separator and downcomer. Heat transfer between the two phases, and between the gas-liquid mixture and cooling coils located in the gas-liquid separator was also accounted for. The model was validated using comparisons of predicted liquid flow rate with the liquid flow rate measured in the downcomer, where a single-phase liquid flow existed. The effects of pressure, current density, number of cells, and bubble size were investigated with the numerical model. The numerical predictions matched the general trends obtained from the experimental results with regard to the effects of pressure and current density on the liquid flow rate. The validated CFD model is being used as a cell design tool at Hydrogenics Corporation.

### 1. INTRODUCTION

The use of fossil fuels as an energy source has resulted in a high concentration level of carbon dioxide in the atmosphere, and consequently the threat of global warming. With continued research and development, hydrogen has the potential to reduce the world's reliance on fossil

fuels in the second half of this century [1]. This would be the first step to the establishment of an envisioned hydrogen economy, where the dominant energy carrier of the economy would be hydrogen that is produced using pollution-free sources [1]. In addition, hydrogen production through water electrolysis is expected to be an enabling technology for increasing utilization of renewable energy sources such as wind and solar power. Electrolysis uses electrical energy to produce hydrogen and oxygen gases from water. Each electrolysis cell consists of a cathode where hydrogen is produced, an anode where the oxygen is produced, and electrolyte in between. In electrolyzers using liquid electrolyte, a microporous medium that allows the flow of ions in the electrolyte, but not of the gases, is placed between the anode and the cathode.

An electrolysis system consists of numerous electrolysis cells, a gas-liquid separator, and the connecting channels. We have developed a numerical model that can be used to predict two-phase flow in an electrolysis system, and thereby the model can be used as an effective design tool for the cell stack and peripherals. Illustrative simulations completed with the numerical model are described in this paper. The model has been successfully used to scale up a commercial alkaline water electrolysis system.

As a first step in the model development, the fundamentals of two-phase flow were studied extensively in order to understand how the gas and electrolyte interact in a water electrolysis cell [2]. This included examining mathematical models that incorporate mass and momentum exchange at the gas-liquid interface in the governing equations, and studying the properties of the different flow regimes that can be formed

in two-phase flow.

Levy [3] provided an overview of this information in his documentation of general two-phase flow in complex systems. Mathematical models specifically representing the two-phase flow in an electrolysis system also were reviewed, along with related experimental results. Mat et al. [4] employed an advanced two-phase flow model to investigate hydrogen evolution in an electrolysis cell operating at atmospheric pressure. Wedin and Dahlkild [5] took a simpler approach when modeling the flow in an electrochemical cell, in which a solution for the transport equations was not needed for both phases. Thorpe et al. [2] conducted an experimental investigation to examine the void fraction and pressure drop in a forced convection water electrolysis cell as a function of the liquid inlet velocity and the current input density. Boissonneau and Byrne [6] continued the experimental analysis on an electrochemical cell to determine the two-phase flow regimes, bubble sizes, gas fractions, and fluid velocities.

In the design of alkaline water electrolysis systems, the gas-liquid circulation flow rate and the gas-liquid separation efficiency are important unknown system parameters playing a significant role in the overall performance. These quantities, which are dependent on the gas-liquid flow patterns, are calculated and analyzed in our gas-liquid flow model using the the solver of general-purpose CFD software, PHOENICS [7]. We have further developed and customized the CFD software to be capable of modeling various two-phase (gas-liquid) flows occurring during hydrogen generation in the whole water electrolysis system under typical and alternative conditions.

A customized computational module, Gas-Liquid flow Analysis and Simulation Software (GLASS), has been developed, tested and validated. GLASS has been successfully used to design system components such as cell stacks, separators and connecting piping (riser and downcomer).

## 2. MODELING APPROACH

The modeling approach applied in this paper is based on modifying the two-fluid inter-phase slip algorithm (IPSA, a built-in modeling option of the PHOENICS software), by adding (user-defined) sub-models describing the complex interaction between the gas and liquid phases in the water electrolysis system. These sub-models account for the bubble size in various system

components. An advanced approach for CFD modeling of gas-liquid flows with user-defined special sub-models is presented below.

It is known that the standard IPSA equations enable a CFD modeler to account for the differences (slips) in velocities and temperatures of gas and liquid in calculation of 3D distributions of pressure, velocity components, temperatures and volume fractions of two phases. The analysis is based on solving the coupled two-fluid conservation equations under typical and alternative operating conditions with appropriate boundary conditions, turbulence models and constitutive inter-phase correlations. In early versions of the CFD model, the drag force between liquid and gas phases was calculated based on the specified average bubble diameter.

Agranat and Tchouvelev [8] found that the basic gas-liquid CFD model based on standard IPSA equations defined in PHOENICS was capable of predicting the gas-liquid flows in separate system components such as a single cell and a gas-liquid separator. However, it was not capable of predicting the flows in the whole electrolysis system, i.e., the cell stack, the separator and the connecting piping. This was due to the fact that, in the standard IPSA equations, the bubble size was assumed to be constant, and the liquid flow rate was assumed to be given.

The integrated CFD model (GLASS) was subsequently developed to simulate the entire electrolysis system. Three geometrical sub-systems of the hydrogen side of the water electrolysis system were considered simultaneously: the horizontal cylindrical gas-liquid separator, the cell stack consisting of cylindrical cells and the connecting piping (riser and downcomer). The primary task of the modeling was to create a cost-effective cell stack design tool that can be utilized without extensive computer hardware or very long computational run times.

In the advanced GLASS developed, the liquid flow rate is a part of solution and the bubble size is considered as a variable, which is calculated using proper correlations accounting for the effects of liquid velocity, gas volume fraction, pressure and geometrical parameters. The appropriate boundary conditions are needed at the gas-liquid inlets and outlets in IPSA analyses. In GLASS, at the gas flow inlets, the gas flow rate,  $Q_G$ , is specified. The liquid flow rate,  $Q_L$ , is automatically calculated during the

CFD runs as the whole electrolysis system is considered and no liquid flow rate specification is needed to solve the CFD equations. At the fluid (liquid and gas) outlets, the outlet boundary conditions are based on specified pressure values.

The list of primary input parameters involved in the CFD modeling of isothermal gas-liquid flows includes the following data:

- Separator/channel/cell geometry, i.e. the dimensions and locations of each CFD object, in particular, inlets, outlets and solid/porous blockages within the fluid domain and at its boundaries.
- Operating pressure and temperature.
- Physical properties of gas and liquid at operating pressure and temperature: densities, viscosities and diffusion coefficients.
- Gas production rate based on the current density and Faraday's law.
- Gas flow rates at the inlets.
- Pressures at the outlets.
- Average bubble size (constant or variable).

The list of output variables obtained from the CFD modeling of isothermal gas-liquid flows includes the following:

- 3D distributions of pressure, gas and liquid velocity components and gas and liquid volume fractions within the computational domain.
- Total gas and liquid flow rates at the outlets from the domain while using the pressure based outlet boundary conditions.

One of the main cell design applications of the CFD analyses is to assess the efficiency of gas-liquid separation within the separator. In particular, the CFD predictions of phase volume fractions,  $\alpha_G$  and  $\alpha_L$ , are important for the analysis of gas-liquid separation efficiency. In the case of 'complete' separation, the values of gas volume fraction,  $\alpha_G$ , at the gas outlet location would be equal to 1 (100%) and, as a result, the values of liquid volume fraction,  $\alpha_L$ , would be equal to zero.

In the case of 'incomplete' separation, the values of  $\alpha_G$  at the gas outlet are smaller than 1 and the values of  $\alpha_L$  are greater than 0. This means that a certain fraction of incoming liquid exits the gas-liquid separator via the gas outlet, i.e., there is some liquid carry-over at the gas outlet. The greater  $\alpha_L$  is at the gas outlet, the lower the gas-liquid separation efficiency.

Another cell design application of CFD modeling is to assess the total liquid (electrolyte) flow rate, which is an unknown parameter in water electrolysis systems based on natural circulation. This quantity affects the performance of the whole electrolysis system, as it affects the cooling capacity of the stack and the gas volume fraction distribution within the electrolysis system. A high liquid flow rate is desired to maximize the cooling capacity of the system.

In this paper, the major focus is on the capability of GLASS to accurately predict the electrolyte flow rate and the liquid to gas flow rate ratio. The latter quantity is a key parameter that is indicative of the cooling capacity of the system and the gas-liquid separation efficiency, and which is governed by the geometry of the system and the resulting flow regimes.

### 3. CFD MODEL FEATURES

A description of the CFD model developed is presented in this section. This includes an overview of the geometry of the system, the input parameters and the models used.

#### 3.1. Electrolysis System Geometry and CFD Model Geometry

The geometry used in the CFD model for the electrolysis system can be seen in Figure 1. This figure displays only the half of the electrolysis system in which hydrogen flows. The electrolysis cells produce the hydrogen that is collected in the top channel. The bottom channel distributes the electrolyte to the numerous electrolysis cells. The bottom channel, electrolysis cells, and top channel represent the electrolysis stack. The collected hydrogen then passes through a riser that connects to the gas-liquid separator. This region allows the hydrogen to flow up to the outlet, while the electrolyte flows down through the downcomer, into the bottom channel of the stack.

Some modifications have been introduced in order to simplify the numerical analysis. The most apparent change involves the use of a symmetry plane across the system, to reduce the simulation time. The riser and downcomer also have square cross sections of the same areas as the circular cross sections in the experimental system, due to the rectangular mesh that was implemented to construct the model. Similarly, the top-to-cell opening and bottom-to-cell opening have rectangular cross sections that have

a similar width as the cells, to significantly reduce the number of elements in the mesh and therefore reduce the simulation time.

Finally, significant modifications to the downcomer were made in the CFD model, to represent the complex downcomer in the actual system. The downcomer simplifications are discussed below.

The actual system that was used for the experiments involves an extremely complex downcomer, with seven bends of various curvatures, and a total length of a few meters. Clearly, the bends and the extra piping will increase the pressure drop, and therefore must be taken into account in the CFD model as an estimated loss coefficient.

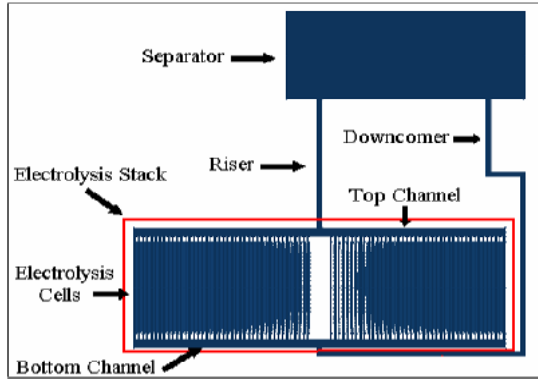


Figure 1: Electrolysis system components.

To incorporate the loss coefficient in the CFD model, an additional quadratic momentum source term must be introduced in the downcomer section of length  $L_c$ , which takes the form of the following equation [7, 9]:

$$\frac{\partial P}{\partial L} = -\rho C V_d^2$$

### 3.2. Two-Phase Governing Equations

The Inter-Phase Slip Algorithm (IPSA), which is a built-in PHOENICS option [7], is used as a framework to incorporate the proper transport equations for the advanced two-phase flow models of GLASS. The IPSA approach is expressed by the following governing equations for mass and momentum, shown below, for the sake of brevity, in the 2D steady-state formulation:

$$\frac{\partial}{\partial x}(\rho_i \alpha_i u_i) + \frac{\partial}{\partial y}(\rho_i \alpha_i v_i) = 0$$

$$\begin{aligned} & \frac{\partial}{\partial x}(\rho_i \alpha_i u_i^2) + \frac{\partial}{\partial y}(\rho_i \alpha_i u_i v_i) \\ &= -\alpha_i \frac{\partial P}{\partial x} + F_r(u_j - u_i) \\ &+ \frac{\partial}{\partial x}\left(\alpha_i \mu_{eff} \frac{\partial u_i}{\partial x}\right) + \frac{\partial}{\partial y}\left(\alpha_i \mu_{eff} \frac{\partial u_i}{\partial y}\right) \\ & \frac{\partial}{\partial x}(\rho_i \alpha_i v_i u_i) + \frac{\partial}{\partial y}(\rho_i \alpha_i v_i^2) \\ &= -\alpha_i \frac{\partial P}{\partial y} + F_r(v_j - v_i) \\ &+ \frac{\partial}{\partial x}\left(\alpha_i \mu_{eff} \frac{\partial v_i}{\partial x}\right) + \frac{\partial}{\partial y}\left(\alpha_i \mu_{eff} \frac{\partial v_i}{\partial y}\right) + F_b \end{aligned}$$

Mat et al. [4] also employed the IPSA approach to simulate two-phase flow in an electrolysis cell. Here, the within-phase turbulent diffusion and the mass diffusion between the two phases at the gas-liquid interface were neglected.

The phase enthalpies,  $H_i$ , are governed by the energy equations

$$\begin{aligned} & \frac{\partial}{\partial x}(\rho_i \alpha_i u_i H_i) + \frac{\partial}{\partial y}(\rho_i \alpha_i v_i H_i) = h_{ij}(T_j - T_i) \\ &+ \frac{\partial}{\partial x}\left(\alpha_i \Gamma_{eff} \frac{\partial H_i}{\partial x}\right) + \frac{\partial}{\partial y}\left(\alpha_i \Gamma_{eff} \frac{\partial H_i}{\partial y}\right) + \dot{S}_{H,i}'''' \end{aligned}$$

The volumetric inter-phase heat transfer coefficients,  $h_{ij}$ , are computed via volumetric inter-phase transfer area, obtained from a spherical liquid/gas fragment diameter, and appropriate Nusselt number.

Heat sources,  $\dot{S}_{H,i}''''$ , occur due to Joule heating in the electrolyte and cooling in the heat exchanger. The phase transformation mass transfer and its thermal effects are assumed to be negligible under the system operational pressures.

The Joule heating rate is given by working voltage, the current density, the number of cells in the stack, and the electrode surface area. The heat transfer in the cooling heat exchanger is expressed in terms of exchanger effectiveness, and then added as a source term to the energy equation for the liquid flow.

The governing equations in the two-phase flow model involve a few parameters that are not solved, and which therefore need to be specified. These parameters include the reference pressure and temperature, the gas and liquid density values, the effective viscosity, and the inter-phase friction; in order to define the inter-phase friction, the drag coefficient and bubble size must also be specified.

It should be mentioned that, in the actual CFD runs, the complete 3D formulation of IPSA was used in both steady state and transient cases.

### 3.3 Operating Conditions and Physical Properties

The pressure of the system at the gas outlet was specified for each simulation. This pressure was used as the reference pressure, and therefore was added to all of the pressure values that were solved by the CFD simulation. It was assumed that the reference pressure was from 5 to 30 bar. The electrolyte density was approximated as  $1265 \text{ kg/m}^3$  (for  $70^\circ\text{C}$  and 30% KOH solution), while the hydrogen gas density,  $\rho_G$ , was obtained according to the operating pressure,  $P$ , and temperature,  $T$ , as:

$$\rho_G = 0.0838 * (P/101330) * 293.15 / (T + 273.15),$$

where pressure is in Pa and temperature is in  $^\circ\text{C}$ . The value of hydrogen gas density is equal to  $0.716 \text{ kg/m}^3$  at 10 bar and  $70^\circ\text{C}$ .

The effective viscosity,  $\mu_{\text{eff}}$ , includes both laminar and turbulent components. The turbulent viscosity was calculated using a modified variant of the LVEL turbulence model in PHOENICS, which accounts for the bubble induced turbulence. The liquid was treated as the nominal carrier phase, and consequently the laminar viscosity of the electrolyte was used to categorize the two-phase flow.

### 3.4. Bubble Size Model

The inter-phase friction term,  $F_r$ , represents the momentum exchange between the two phases. The dispersed flow drag model, shown in the following equation is used, which relates the inter-phase friction to the drag coefficient,  $c_d$ , and bubble size,  $d_b$ :

$$F_r = 0.75 \frac{c_d \rho_L \alpha_L \alpha_G}{d_b} |V_r|$$

where  $V_r$  is the slip velocity vector between the two phases.

The drag model that was implemented to determine the drag coefficient,  $c_d$ , assumes that the gas bubbles are spherical, and that the drag is a function of the Reynolds number based on the bubble size [7].

The bubble size,  $d_b$ , is an important parameter that affects the overall liquid flow rate and the volume fraction of the hydrogen. The electrolysis system is separated into four parts, in which the bubble size in each part is specified by different correlations based on the hydrogen volume fraction at the location. The four parts of the system are as follows: the liquid inlet, the bottom channel, and the bottom-to-cell openings; the cells; the top-to-cell openings, the top channel, and the riser; and the separator and the gas outlet.

### 3.5. Boundary Conditions

To simulate the flow in the electrolysis system, proper boundary conditions that govern the gas production rate must be specified. Also, proper liquid inlets must be introduced to ensure that the system is at steady state.

To determine the hydrogen gas production rate, the current density must first be determined. The current density,  $i$ , is assumed to be constant over the electrode surface, as in the model of Wedin and Dahlkild [5]. With the current density known, Faraday's law, shown in the following equation, can be used to determine the horizontal inlet velocity component of the hydrogen gas,  $u_{GI}$ , which leaves the cathodes:

$$u_{GI} = \frac{1}{2} \frac{R(T + 273.15)}{P} \frac{i}{F},$$

$$F = 96487 \text{ C/mol}, R = 8.314 \text{ J/molK}$$

Using the above equation, the hydrogen gas generation rate at the gas inlet (the cathode),  $Q_{GI}$ , is obtained under the given conditions of operating pressure, temperature, electric current density,  $i$ , and cathode surface area,  $A$ :

$$Q_{GI} = 0.4184 \frac{1}{3600} \frac{101330(T + 273.15)}{P * 273.15} \frac{iA}{1000}$$

Here, the gas generation rate is calculated in  $\text{m}^3/\text{s}$ ,  $T$  is in  $^\circ\text{C}$ ,  $P$  is in Pa,  $i$  is in  $\text{A/m}^2$  and  $A$  is in  $\text{m}^2$ .

Representation of the gas-liquid separation process was accomplished by introducing a liquid inlet that provides the same mass flow as the liquid leaving the system through the gas outlet (cyclic boundary conditions). At the fluid

(liquid and gas) outlets, the outlet boundary conditions were based on specified pressure values.

#### 4. MODEL VALIDATION

The simulation results obtained with the basic CFD model by Agranat and Tchouvelev [8] were validated by comparing PHOENICS modeling results with the experimental data of Thorpe et al. [2] for a low-pressure rectangular electrolysis cell. PHOENICS predictions of the hydrogen volume fraction compared well with the results reported by Thorpe et al.

To further develop and validate the CFD models (basic and advanced), experimental flow rate data were obtained under high-pressure conditions (5 bars) in the range of current densities from 1 to 4 kA/m<sup>2</sup> using a liquid flow meter installed in the downcomer line (see Figure 1), where the single phase flow conditions were observed and predicted. Liquid flow rate, which is one of the key parameters, was calculated using the GLASS model and then measured at the downcomer line.

A comparison of the experimental and numerical results indicated that the numerical model over predicted the liquid flow rates by approximately 6%. The error in the predicted flow rates may have been due to the fact that the numerical model did not consider many aspects present in the physical system, such as the porous medium in the cells, the heat exchanger in the gas-liquid separator, and heat transfer aspects. There were also numerous simplifications implemented into the CFD model geometry that would result in a larger predicted flow rate (see CFD model description above).

The computations were performed with the non-uniform grid of 250,000 cells. Although it is almost certain that the results are not yet fully grid-independent, the relevant studies performed for separate system units, indicate that the effects of further refinement on the circulation flow rate may be quite small. Overall indeed, a comparison of the results obtained by number of different grids reveals some local differences considered to be acceptable from practical point of view.

#### 5. SIMULATION RESULTS

Results of CFD modeling were obtained with the GLASS module for Hydrogenics' existing

cell stack system (hydrogen side) under typical operating conditions. The total liquid flow rate and the 3D distribution of gas volume fraction were calculated for the entire electrolysis system. A sensitivity study was conducted to analyze the effects of operating conditions on the liquid flow rate and efficiency of gas-liquid separation. The separation efficiency was assessed based on the 3D distribution of the gas volume fraction within the separator vessel and the percentage of liquid carry-over at the gas outlet. The effects of pressure, current density, number of cells, and bubble size were investigated with the numerical model.

Figure 2 shows the effect of current density on the hydrogen volume fraction predicted at the riser (riser voidage) of the cell stack. The effect of the current density on the two-phase flow characteristics was determined by varying the current density from 2 kA/m<sup>2</sup> to 6 kA/m<sup>2</sup> under different operating pressures. In terms of gas-liquid flow, it would be beneficial to operate the electrolysis system at a higher pressure and a lower current density, as the void fraction at the riser is lower in those cases. Figure 3 shows the effect of current density on the liquid to gas flow rate ratio predicted for the cell stack. The trends obtained from the experimental analysis with regard to the effects of pressure and current density on the liquid flow rate matched the numerical model predictions.

Also, sensitivity runs were performed in order to analyze the sensitivity of the CFD predictions with respect to the bubble size model parameters. The model predicted a maximum decrease of 15% in the liquid flow rate due to larger hydrogen bubbles. This indicates that the bubble size can have a significant effect on the two-phase flow in the system.

While the hydrodynamic model has been used in a whole-domain manner to represent the separation, the heat transfer module has been applied to cover the part of the domain below the phase inversion surface.

The inspection of computed phase temperature fields in the system reveals that the temperatures of the liquid and gas are very close. The highest temperatures are predicted next to the exits from the cells, and they decrease to the lowest values in the downcomer. This is due to the fact of cooling in the heat exchanger. It has also become evident that the temperatures are distributed non-uniformly in gas-evolving cell assembly.

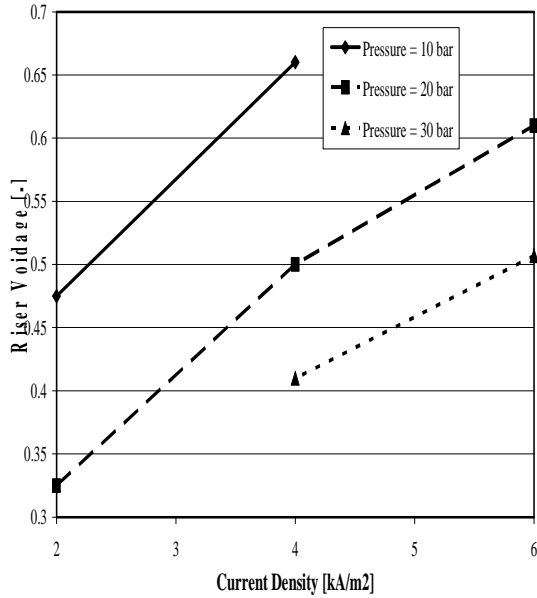


Figure 2: Effect of current density on riser voidage for a cell stack.

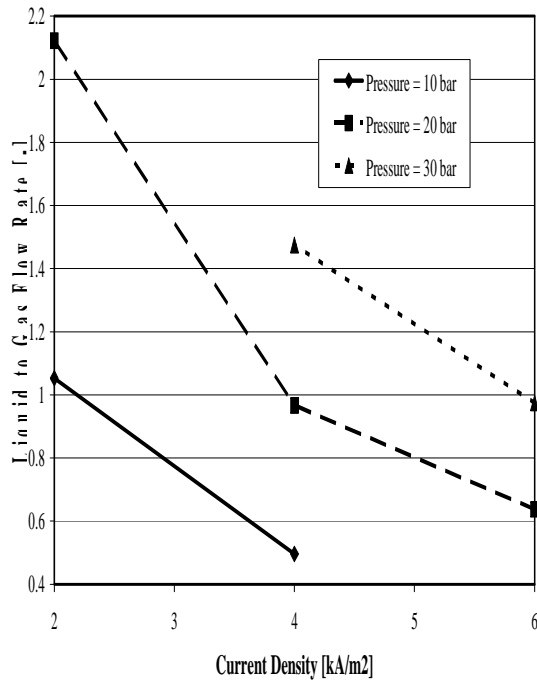


Figure 3: Effect of current density on liquid to gas flow rate ratio for a cell stack.

The inspection of the distributions in cross sections of the system indicates, as expected, that the temperature fields exhibit well pronounced circumferential variations. No well-mixed state is achieved in cell assembly, and three-dimensionality is observed everywhere in the

stack system except connecting passages. Further inspection of the results obtained show that all results indicate correct trends.

The model developed is seen as an effective method of prediction of fluid flow and heat transfer in water electrolysis system. In addition to gas and liquid flows, detailed heat transfer calculations can be performed. The predictions provide the detailed information for each phase regarding the three dimensional two-phase fields of velocity, temperature, pressure, and void fractions.

## 6. CONCLUSIONS

The PHOENICS CFD software has been appropriately modified for modeling the gas-liquid flows and heat transfer in water electrolysis systems, including the hydrogen generation cell stacks, gas-liquid separator and external connecting piping. A customized module, GLASS, has been developed, validated and applied to the commercial system configuration under typical operating conditions. The modeling results indicate significant sensitivity of liquid flow rate and separation efficiency to the bubble size and operating conditions. The advanced CFD model has been validated against experimental data and is being used as a cost-effective and reliable design tool. The model predictions clearly show the effects of alternative operating conditions and/or geometrical parameters on the gas-liquid flow characteristics and the electrolysis system performance.

## ACKNOWLEDGEMENTS

The authors gratefully acknowledge the financial support of Natural Resources Canada (NRCan) for part of this work.

## NOMENCLATURE

C	Coefficient of source term, 1/m	y	Vertical coordinate, m
$c_d$	Drag coefficient	z	Horizontal coordinate, m
$d_B$	Bubble diameter, m		
F	Faraday's constant, C/mol		
$F_b$	Buoyancy force, $\text{kg}/(\text{m}^2\text{s}^2)$	Greek Letters	
$F_r$	Friction coefficient, $\text{kg}/(\text{m}^3\text{s})$	$\alpha$	Volume fraction
g	Gravitational constant, $\text{m}/\text{s}^2$	$\mu_{\text{eff}}$	Effective viscosity, $\text{kg}/\text{m}\cdot\text{s}$
i	Current density, $\text{A}/\text{m}^2$	$\nu_L$	Liquid kinematic viscosity, $\text{m}^2/\text{s}$
k	Liquid to gas flow rate ratio	$\rho$	Density, $\text{kg}/\text{m}^3$
$L_C$	Length of downcomer where C is applied, m	$\sigma_L$	Liquid surface tension, N/m
P	Pressure, Pa		
R	Universal gas constant, J/(molK)		
T	Temperature of liquid-gas mixture, °C		
u	x-velocity component, m/s		
$u_{GI}$	Cell gas inlet velocity, m/s	Subscripts	
v	y-velocity component, m/s	G	Property for gas phase
$V_r$	Slip velocity vector	i	Property for either liquid or gas phase
$V_d$	Average velocity in downcomer	I	Property at gas inlet
w	z-velocity component, m/s	j	Property for either liquid

			or gas phase
X	Horizontal coordinate, m	L	Property for liquid phase

## REFERENCES

- Romm, J. J. 2004. The hype about hydrogen. Issues in Science and Technology, Vol. 20, No. 3, pp. 74-81.
- Thorpe, J.F., J.E. Funk, and T.Y. Bong. 1970. Void fraction and pressure drop in a water electrolysis cell. Journal of Basic Engineering, Transactions of the ASME, March: pp. 173-182.
- Levy, S. 1999. Two-Phase Flow in Complex Systems. New York: John Wiley & Sons.
- Mat, M., K. Aldas, and O. Ilegbusi. 2004. A two-phase flow model for hydrogen evolution in an electrochemical cell. International Journal of Hydrogen Energy, Vol. 29, pp. 1015-1023.
- Wedin, R. and A. Dahlkild. 2001. On the transport of small bubbles under developing channel flow in a buoyant gas-evolving electrochemical cell. Industrial and Engineering Chemical Research, Vol. 40, pp. 5228-5233.
- Boissonneau, P. and P. Byrne. 2000. An experimental investigation of bubble-induced free convection in a small electrochemical cell. Journal of Applied Electrochemistry, Vol. 30, pp. 767-775.
- PHOENICS Documentation (Version 3.5). 2002. Concentration, Heat and Momentum Limited, London, UK.
- Agranat, V. and A. Tchouvelev. 2004. CFD modeling of gas-liquid flows in water electrolysis units. In Proceedings of 15<sup>th</sup> World Hydrogen Energy Conference. Yokohama, Japan.
- White, F. 2003. Fluid Mechanics, Fifth Edition, New York: The McGraw-Hill Companies.